European Journal of Medicinal Chemistry 137 (2017) 76–87

Contents lists available at ScienceDirect

European Journal of Medicinal Chemistry

journal homepage: http://www.elsevier.com/locate/ejmech

Research paper

New bicyclic brominated furanones as potent autoinducer-2 quorum-sensing inhibitors against bacterial biofilm formation

Ji Su Park [a, 1], Eun-Ju Ryu [b, 1], Linzi Li [a], Bong-Kyu Choi [b, **], B. Moon Kim [a, *]

[a] Department of Chemistry, College of Natural Sciences, Seoul National University, 1 Gwanak-ro, Gwanak-gu, Seoul 08826, Republic of Korea
[b] Department of Oral Microbiology and Immunology and Dental Research Institute, School of Dentistry, Seoul National University, 101 Daehak-ro, Jongno-gu, Seoul 03080, Republic of Korea

ARTICLE INFO

Article history:
Received 1 February 2017
Received in revised form
12 May 2017
Accepted 14 May 2017
Available online 17 May 2017

Keywords:
Quorum sensing
Bacterial biofilm
AI-2 inhibitors
Brominated furanones

ABSTRACT

Bacterial behaviors such as virulence factor secretion and biofilm formation are critical for survival, and are effectively regulated through quorum sensing, a mechanism of intra- and interspecies communication in response to changes in cell density and species complexity. Many bacterial species colonize host tissues and form a defensive structure called a biofilm, which can be the basis of inflammatory diseases. Periodontitis, a chronic inflammatory disease affecting the periodontium, is caused by subgingival biofilms related to periodontopathogens. In particular, *Fusobacterium nucleatum* is a major co-aggregation bridge organism in the formation and growth of subgingival biofilms, linking the early and late colonizers in periodontal biofilms. According to our previous study, the intergeneric quorum-sensing signal molecule autoinducer-2 (AI-2) of *F. nucleatum* plays a key role in intra- and interspecies interactions of periodontopathogens, and may be a good target for periodontal biofilm inhibition. Recently, brominated furanones produced by the macroalga *Delisea pulchra* were shown to inhibit biofilm formation via AI-2, and have been investigated toward the goal of increasing the inhibition effect. In this study, we describe the synthesis of new bromofuranone analogs, i.e., 3-(dibromomethylene)isobenzofuran-1(3H)-one derivatives, and demonstrate their inhibitory activities against biofilm formation by periodontopathogens, including *F. nucleatum, Porphyromonas gingivalis, and Tannerella forsythia.*

1. Introduction

Quorum sensing (QS) is the process of cell-to-cell communication in microorganisms mediated by small signaling molecules referred to as autoinducers, which are secreted by bacteria and fungi [1–3]. Bacteria can effectively regulate numerous phenotypes, including virulence factor expression, bioluminescence, and biofilm formation, in response to their changes in population density through recognition of the threshold reached by autoinducers, the so-called quorum, via intracellular or intercellular communication [4]. In particular, formation of a biofilm can not only enhance the viability of bacteria in response to antibiotics but can also be the basis of the development of chronic inflammatory diseases, including endocarditis, cystic fibrosis, osteomyelitis, chronic urinary tract infections, chronic prostatitis, and periodontal diseases [5].

QS molecules can be classified into three major types: oligopeptides, acyl-homoserine lactones (AHLs, autoinducer-1), and autoinducer-2 (AI-2). Oligopeptides and AHLs are used by gram-negative and gram-positive bacteria, respectively, in intraspecies communication [6]. AI-2 is a universal QS molecule secreted by both gram-negative and gram-positive bacteria [7–9], and plays a critical role in the virulence of pathogenic bacteria and in biofilm formation [10]. AI-2 mediates both intra- and interspecies communication, and can thus be a good target for the regulation of bacterial infection. Accordingly, AI-2 inhibitors are ideal compounds for bacterial biofilm inhibition in multispecies bacterial communities.

More than 700 species of bacteria have been found in the human oral cavity, which establish mixed-species communities [11]. Among these oral bacteria, periodontopathogens, including *Aggregatibacter actinomycetemcomitans*, *Fusobacterium nucleatum*, *Porphyromonas gingivalis*, *Tannerella forsythia*, and spirochetes, form subgingival biofilms and cause periodontitis, which is a

* Corresponding author.
** Corresponding author.
E-mail addresses: bongchoi@snu.ac.kr (B.-K. Choi), kimbm@snu.ac.kr (B.M. Kim).
[1] These two authors contributed equally to this work.

http://dx.doi.org/10.1016/j.ejmech.2017.05.037
0223-5234/

chronic inflammatory disease. Since AI-2 is an interspecies QS molecule that controls intergeneric signaling, it may induce oral biofilm formation and increase the bacterial virulence of periodontopathogens [12–14]. Furthermore, Kolenbrander et al. [15] suggested that, compared to commensal bacteria, periodontopathogens produce much higher levels of AI-2; such high concentrations would enhance pathogen biofilm maturation, leading to periodontitis. In particular, *F. nucleatum* is known as a major co-aggregation bridge organism that connects late pathogenic colonizers and early commensal colonizers in a periodontal biofilm [15–19]. We previously reported that the level of *F. nucleatum* AI-2 was reduced by QS inhibitors (QSIs), including (5Z)-4-bromo-5-(bromomethylene)-2(5H)-furanone and D-ribose [20]. Because of the diversity of oral bacteria, it is hard to selectively eliminate periodontopathogens without disturbing oral commensals. Therefore, oral biofilm formation regulation using QSIs is one of the most hopeful protective means for preserving oral health [21].

Brominated furanones produced from the macroalga *Delisea pulchra* are known to prevent microbial colonization [22,23]. In addition, these compounds have been shown to inactivate LuxS, which is required for AI-2 synthesis, and to inhibit the QS activity of various bacterial species [4,24–27]. Recently, Yang et al. [28] reported a bicyclic version of brominated furanones that could potentially reduce their toxicity while retaining their biofilm inhibitory activities. However, compared with reported monocyclic brominated furanones, the inhibitory activities of the bicyclic furanones were relatively low [28]. These results suggest that modification of the exocyclic vinyl position, which is an essential structural element for the inhibition of LuxS [29], is not an appropriate strategy for the development of effective QSI's. Therefore, discovery of new potent and safer brominated furanone candidates is still desired. In this study, to improve the QS inhibitory activity and biofilm inhibition efficacy of periodontal bacteria, we report the synthesis and evaluation of 3-(dibromomethylene)isobenzofuran-1(3H)-one derivatives, which have different ring sites from the existing bicyclic compound. In particular, we investigated the structure-activity relationships of the biofilm inhibition effects of various new furanone derivatives prepared with new ring structures and possible side chains on the new ring.

2. Results and discussion

2.1. Chemistry

We focused on the design and synthesis of new bicyclic brominated furanone derivatives with reduced toxicity while retaining or enhancing their biofilm inhibitory activities. As shown in Table 1, we synthesized two kinds of bicyclic brominated furanone derivatives: one through the modification of the ring structure and the other through introduction of a side chain onto the benzene ring. The ring structural component of furanones has been reported to be important for the inhibition of biofilm formation by bacteria [28]. Thus, compounds with different ring structures (**1**–**5**) were designed for evaluation of the ring structure effect on the biofilm inhibitory activity. Another set of compounds possessing side chains on the benzene ring (**6**–**9d**) were designed with the aim of investigating the influence of the side chain length on the benzene ring, since previous reports have shown that monocyclic furanones with chain lengths of two to six atoms show good inhibitory activities [30,31].

According to the Ramirez olefination procedure [32], brominated compounds with various ring structures (**10**–**14**) shown in Table 1 were synthesized from the corresponding commercially available compounds in one step. The yields of the products ranged from low to moderate (14–65% yields). Although the reactions proceeded for cyclopropane- and cyclobutane-1,2-dicarboxylic anhydrides, the olefination products decomposed rapidly at room temperature, presumably due to the unstable nature of the anhydrides based on the angle strains of the hydrocarbon ring [33].

For the preparation of brominated furanone derivatives containing alkoxy groups on the benzene ring, such as **16a**–**16e** and **18a**–**18d**, starting materials containing the alkoxy derivatives **7a**–**7e** and **9a**–**9d** were prepared from the corresponding phenol derivatives through the use of a reported synthetic method [34]. These precursors (**7a**–**7e** and **9a**–**9d**) were obtained at moderate to good yields over four steps (45–77%). Through the Ramirez olefination with anhydrides possessing side chains on the benzene ring (**6**–**9d**), brominated compounds **15**–**18d** were produced with 70–83% regioselectivity. Similar to a study that examined the regioselectivity of Wittig reactions for mono-substituted phthalic anhydrides [35], this result showed that the electronic effects of the substituents appear to have a large influence on the regioselectivity of the olefination. Brominated compounds **15**–**18d** were obtained in overall yields ranging from 16% to 22%. Although small amounts of minor regioisomers were produced in olefination with the anhydrides **6**–**9d,** we focused on the major product because of its better inhibitory effect on biofilm formation. All target compounds were separated and purified through the use of column chromatography. The structures of the desired products were confirmed by spectroscopic analyses, including ^{1}H, ^{13}C, heteronuclear multiple bond correlation (HMBC), and mass spectrometry (MS).

2.2. Biological evaluation

In our preliminary experiments, in order for us to evaluate the inhibitory activities based on the ring structural component of the inhibitors, brominated furanone compounds with different ring structures (**10**–**14**) were screened for their inhibitory effects on the biofilm formation of *F. nucleatum* at 0.2 and 2 μM concentrations (Fig. S1). Since it was confirmed in previous studies that the reference furanone compound **R1**, (*Z*)-4-bromo-5-(bromomethylene)furan-2(5H)-one, has neither bactericidal effect nor cytotoxicity against host cells at 2 μM [20], the following experiments were performed starting at 2 μM. As shown in Fig. S1, bromofuranones containing a benzene ring (**10**) and a 5-membered ring (**13**) showed higher inhibitory activities at 0.2 and 2 μM compared to other compounds examined.

According to previous reports [30,31], the biofilm inhibitory activities of furanones were dependent on the side chain structure. Therefore, we synthesized brominated furanone derivatives (**15**–**18d**) based on compound **10**, which showed good inhibitory activity, and investigated the biofilm inhibitory effects according to the variation of the side chains. Compounds **15**–**18d** were evaluated along with compounds **10**–**14** at 0.02 and 0.2 μM to investigate the activities at lower concentrations. Compounds with 5-membered ring structure (**13**) and a short side chain on the benzene ring (**15** and **17**) showed high inhibitory effects on the biofilm formation of *F. nucleatum*. However, as shown in Fig. S2, the inhibitory activities of compounds except for **13**, **15** and **17** were worse than that of compound **R1** as the increase of the chain length rather decreased the inhibitory activity.

2.2.1. Inhibitory effect of new furanone compounds on AI-2 activity

To investigate whether the inhibitory effects of highly active compounds (**13**, **15** and **17**) on biofilm formation arise from the inhibition of AI-2 activity, these furanone compounds were evaluated for their inhibitory activities on the AI-2 activity at 2 μM. AI-2 activities were assessed using *Vibrio harveyi* BB170, an AI-2 reporter strain, by measuring the AI-2-mediated bioluminescence of the

Table 1
Synthesis of bicyclic brominated furanone derivatives.

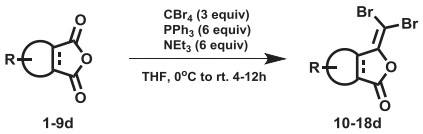

Entry	Substrate	Product	Yield (%)[a]
1	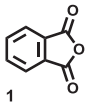 **1**	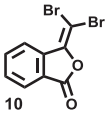 **10**	30%
2[b]	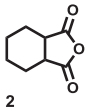 **2**	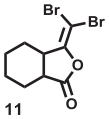 **11**	14%
3	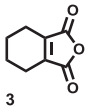 **3**	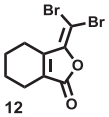 **12**	65%
4	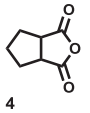 **4**	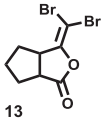 **13**	21%
5	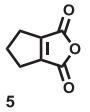 **5**	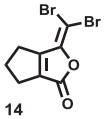 **14**	27%
6	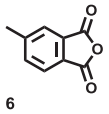 **6**	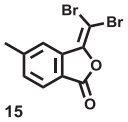 **15**	24%
7	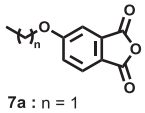 **7a** : n = 1 **7b** : n = 2 **7c** : n = 3 **7d** : n = 4	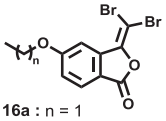 **16a** : n = 1 **16b** : n = 2 **16c** : n = 3 **16d** : n = 4	**16a** : 20% **16b** : 19% **16c** : 21% **16d** : 19%
8	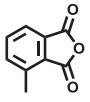 **8**	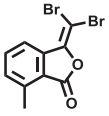 **17**	26%
9	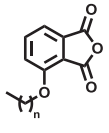 **9a** : n = 1 **9b** : n = 2 **9c** : n = 3 **9d** : n = 4	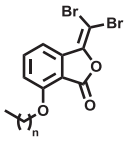 **18a** : n = 1 **18b** : n = 2 **18c** : n = 3 **18d** : n = 4	**18a** : 19% **18b** : 18% **18c** : 18% **18d** : 16%

[a] Yields of isolated products
[b] Absence of triethylamine

bacteria. As shown in Fig. 1, compounds **13**, **15**, and **17** at 2 μM significantly reduced the bioluminescence of *V. harveyi* BB170 induced by *F. nucleatum* AI-2, but their inhibitory activities appeared to be lower than that of the compound **R1** (Fig. 1A).

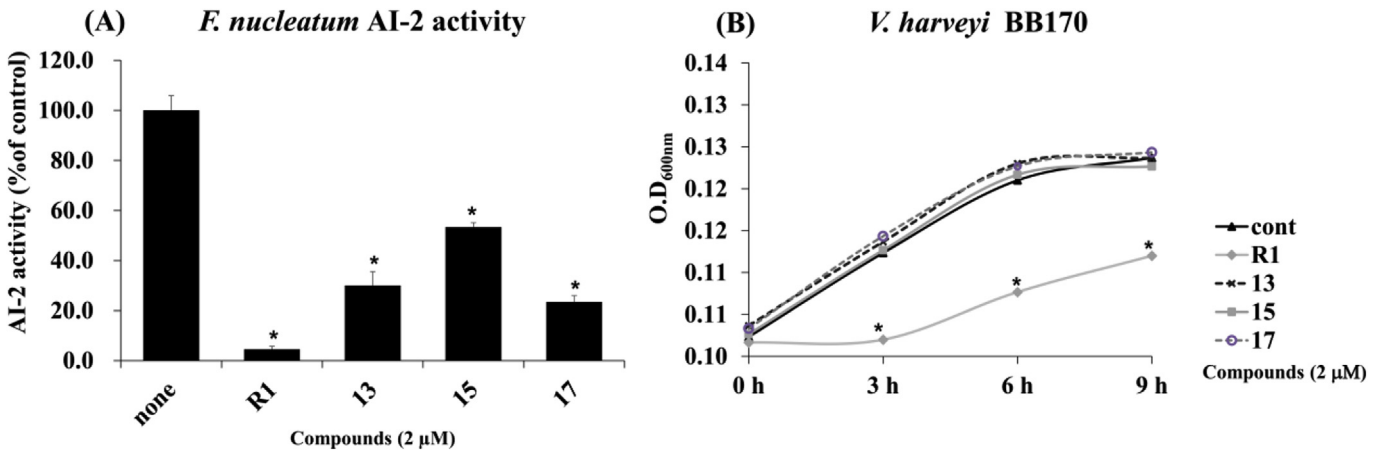

Fig. 1. Effect of furanone compounds on AI-2 activity and *V. harveyi* growth. (A) AI-2 activity was assessed by measuring bioluminescence using the AI-2 reporter strain *V. harveyi* BB170. *V. harveyi* BB170 (1×10^6 bacteria/mL) was incubated for 6 h with 10% semi-purified *F. nucleatum* AI-2 in the absence or presence of furanone compounds (**13**, **15**, and **17**) and the reference furanone compound (**R1**) at a concentration of 2 μM. The bioluminescence of *V. harveyi* BB170 was measured using a luminometer and the value was converted to a percentage of the control value. $^*p < 0.05$ compared to the value of the *F. nucleatum* AI-2-treated group. (B) *V. harveyi* BB170 was grown aerobically for 9 h in the absence of *F. nucleatum* AI-2 at 30 °C in the presence of the reference furanone compound (**R1**) or new furanone compounds (**13**, **15**, and **17**) at a concentration of 2 μM. Planktonic bacterial growth was monitored by measuring absorbance at 600 nm using a spectrophotometer. $^*p < 0.05$ compared to the untreated group (cont). The experiments were performed three times in triplicate and representative data are shown.

Through an additional bacterial growth test, we confirmed that the compound **R1** significantly inhibited the growth of *V. harveyi* BB170 (Fig. 1B), resulting in the reduction of bioluminescence. However, the newly synthesized furanone compounds did not affect the planktonic growth of *V. harveyi* BB170. This revealed that the inhibitory effect of highly active compounds on biofilm formation was caused by inhibition of the AI-2 activity without affecting the planktonic growth of *V. harveyi* BB170.

Through *F. nucleatum* biofilm formation assay and AI-2 activity test, it was found that 5-membered ring structure (**13**) and benzene derivatives having a short side chain (**15** and **17**) exhibit good inhibitory effects on biofilm formation through the inhibition of AI-2 activity. Therefore, three most effective compounds (**13**, **15** and **17**) were selected.

2.2.2. Inhibitory effect of the new furanone compounds on the biofilm formation of major periodontopathogens

To evaluate the biofilm formation inhibitory effect of the three new furanone compounds (**13**, **15**, and **17**) with high inhibitory activity on the major periodontopathogens, *F. nucleatum, P. gingivalis*, and *T. forsythia* were grown on a cover slip in the absence or presence of the compounds, followed by observation using a confocal laser-scanning microscope. The biofilm formed by each group was also analyzed by measuring the biomass and average thickness. As shown in Fig. 2 and Table 2, the furanone compounds **13**, **15**, and **17** at a concentration of 2 μM remarkably reduced the biofilm formation of periodontopathogens induced by *F. nucleatum* AI-2. The biomass of the biofilm formed by *F. nucleatum, P. gingivalis*, and *T. forsythia* was quantified by dividing the value of the total fluorescence intensity by the area after culture alone or with 10% semi-purified *F. nucleatum* AI-2 in the absence or presence of the compound **R1** or new furanone compounds (**13**, **15**, and **17**) at 2 μM. The average depth of the biofilm formed on glass cover slips was analyzed using the Carl Zeiss LSM 700 program. The inhibitory effects of all three compounds on the biofilm formation of *F. nucleatum*, *P. gingivalis*, and *T. forsythia* were comparable to those of the compound **R1**.

To assess the effects of the compounds at lower concentrations, the biofilm formation was evaluated by crystal violet staining. As shown in Fig. 3, compounds **13**, **15**, and **17** significantly reduced the biofilm formation of *F. nucleatum*, *P. gingivalis*, and *T. forsythia* induced by *F. nucleatum* AI-2. Compounds **13**, **15**, and **17** significantly inhibited the biofilm formation of *F. nucleatum*, and their inhibitory activities were higher at all concentrations tested (0.002–2 μM) than that of the compound **R1**. In the case of *P. gingivalis*, compound **17** showed a higher inhibitory effect on biofilm formation than the compound **R1** at all concentrations tested, whereas compounds **13** and **15** showed higher inhibitory activity at the concentration of 0.02 μM and 0.2 μM, respectively. Compared to the compound **R1**, compounds **17**, **13**, and **15** showed higher inhibitory activity of *T. forsythia* biofilm formation at 0.002–0.2 μM, 0.2 μM, and 0.2 and 2 μM, respectively. The inhibitory activities of compounds **13** and **17** did not follow a dose-dependent tendency, which varied according to the bacterial species. Although AI-2 is a universal signaling molecule, the structure of the AI-2 receptor may be slightly different among bacterial species [4,36]. The furanone compounds may act as partial agonists or antagonists depending on the concentration in accordance with the different structures of AI-2 receptors [37–39]. AI-2 receptors or transporters have been reported in several species of bacteria, including LsrB and LsrR in *Escherichia coli* and *Salmonella* Typhimurium, AgrC in *Staphylococcus aureus*, TlpB in *Helicobacter pylori*, and LuxP/Q in *Vibrio* sp. [40]. However, the AI-2 receptors of periodontopathogens have only been reported in *A. actinomycetemcomitans* [41,42]. To clarify the interaction between the receptors and their ligands, the structure of an AI-2 sensor in periodontopathogens needs to be identified. Furthermore, the inhibitors may inhibit other adhesin-related factors of periodontopathogens induced by AI-2, resulting in further inhibition of biofilm formation; this hypothesis also remains to be tested. It is notable that the inhibitory activities of **13**, **15**, and **17** against *F. nucleatum* biofilm formation are superior to those of the reference furanone compound **R1** at a concentration as low as 2 nM. As *F. nucleatum* mediates the colonization of periodontopathogens, including *P. gingivalis*, *T. forsythia,* and *Treponema denticola*, the inhibition of biofilm formation can hamper the development of a pathogenic biofilm, and thus prevent periodontitis [19,20,43,44].

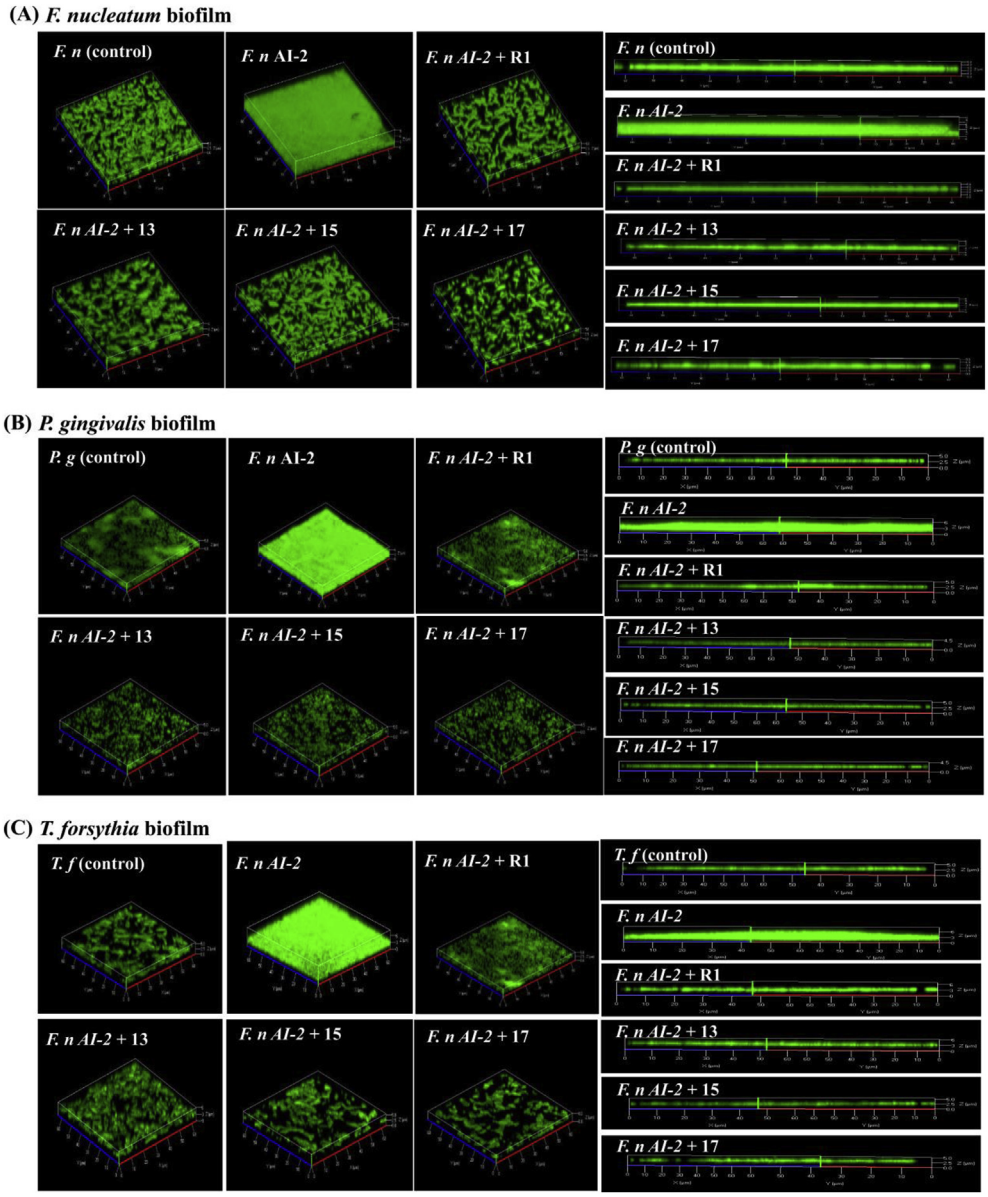

Fig. 2. Biofilm images showing the inhibitory effects of furanone compounds on the biofilm formation of *F. nucleatum*, *P. gingivalis*, and *T. forsythia*. (A) *F. nucleatum* (2×10^7 bacteria/mL), (B) *P. gingivalis* (2×10^8 bacteria/mL), and (C) *T. forsythia* (2×10^8 bacteria/mL) were cultured with semi-purified *F. nucleatum* AI-2 in the absence or presence of the reference furanone compound (**R1**) or new furanone compounds (**13**, **15**, and **17**) at 2 μM under an anaerobic condition at 37 °C. After 48 h incubation, each biofilm formed on glass cover slips was stained with the live/dead-BacLight bacterial viability kit followed by observation using a confocal laser-scanning microscope at 1000× magnification. The control group was the biofilm of each bacterium cultured without *F. nucleatum* AI-2 and inhibitors.

Table 2
Biomass and depth of periodontopathogen biofilms.

Bacteria / Treatment	*F. nucleatum*		*P. gingivalis*		*T. forsythia*	
	Biomass ($\mu m^3/\mu m^2$)	Average Depth (μm)	Biomass ($\mu m^3/\mu m^2$)	Average Depth (μm)	Biomass ($\mu m^3/\mu m^2$)	Average Depth (μm)
Control	0.43	2.11	0.37	2.06	0.52	2.21
Fn AI-2	2.99*	5.37*	3.73*	4.87*	4.05*	5.29*
Fn AI-2/ R1	0.42#	2.02#	0.30#	2.05#	0.77#	2.18#
Fn AI-2/ 13	0.39#	1.82#	0.31#	2.05#	0.93#	2.27#
Fn AI-2/15	0.38#	1.87#	0.29#	2.05#	0.59#	1.94#
Fn AI-2/ 17	0.32#	1.72#	0.27#	1.97#	0.88#	2.41#

*$p < 0.05$ compared with the untreated group (Control), and #$p < 0.05$ compared with the *F. nucleatum* AI-2-treated value in the absence of furanone compounds

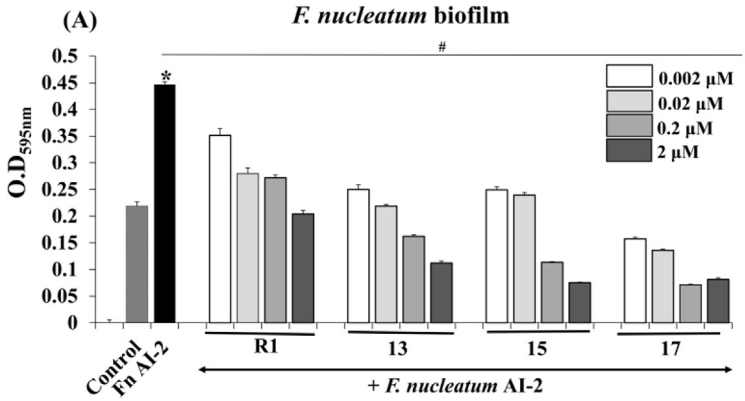

	Biofilm formation (%)			
	0.002 μM	0.02 μM	0.2 μM	2 μM
Fn AI-2	100	100.00	100	100
R1	82.56	69.51	68.05	55.61
13	64.02	58.29	47.93	38.78
15	63.90	62.07	39.02	32.07
17	47.07	43.17	31.34	33.17

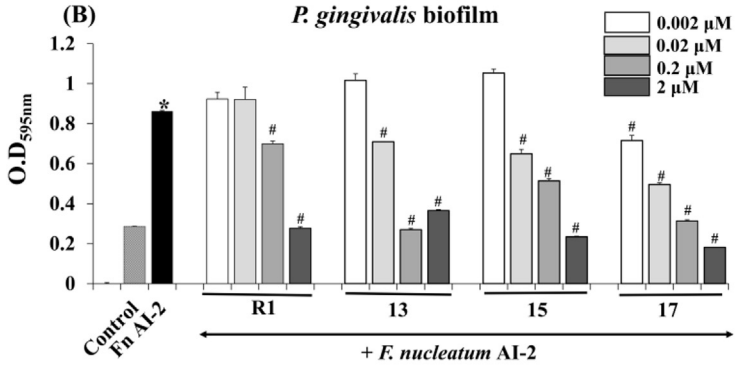

	Biofilm formation (%)			
	0.002 μM	0.02 μM	0.2 μM	2 μM
Fn AI-2	100	100.00	100	100
R1	106.31	106.10	83.09	39.22
13	116.08	84.13	38.46	48.37
15	119.89	77.89	63.83	34.72
17	84.75	61.95	42.97	29.31

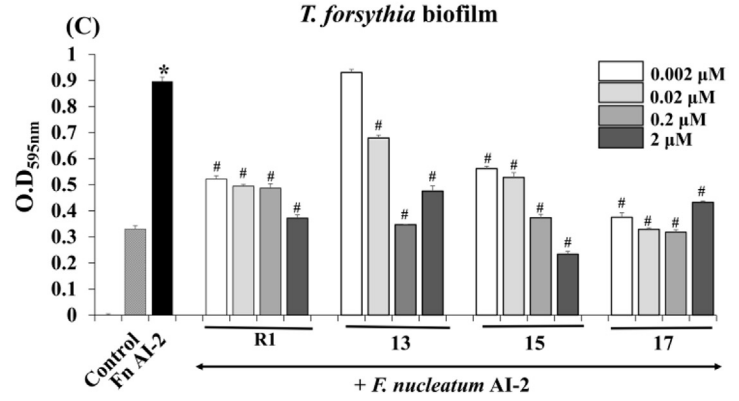

	Biofilm formation (%)			
	0.002 μM	0.02 μM	0.2 μM	2 μM
Fn AI-2	100	100.00	100	100
R1	62.45	59.71	58.90	47.39
13	103.41	78.18	44.85	57.76
15	66.40	63.05	47.52	33.47
17	47.66	43.04	41.97	53.48

Fig. 3. Inhibitory effects of furanone compounds on the biofilm formation of periodontopathogens at various concentrations. (A) *F. nucleatum* (2×10^7 bacteria/mL), (B) *P. gingivalis* (2×10^8 bacteria/mL), and (C) *T. forsythia* (2×10^8 bacteria/mL) were cultured with 10% semi-purified *F. nucleatum* AI-2 in the presence of the reference furanone compound (**R1**) or new furanone compounds (**13**, **15**, and **17**) at various concentrations for 48 h. Biofilm formation was assessed by crystal violet staining. *$p < 0.05$ compared with the non-treated value, and #$p < 0.05$ compared to the *F. nucleatum* AI-2-treated value in the absence of furanone compounds. The experiments were performed three times in triplicate and representative data are shown.

2.2.3. Effect of the new furanone compounds on planktonic bacterial growth

Traditional antibacterial agents aim to kill or inhibit bacterial growth. However, QSIs generally target virulence expression without bacterial growth inhibition. To confirm whether the inhibitory effect of the new furanone compounds on the biofilm formation of periodontopathogens is not attributed to bacterial growth inhibition, we assessed the effects of the compounds on planktonic bacterial growth. As shown in Fig. 4, the compounds did not inhibit the growth of *F. nucleatum*, *P. gingivalis*, and *T. forsythia* at the highest concentration tested (2 μM) in the biofilm formation assay.

2.2.4. Cytotoxicity evaluation of the new furanone compounds

To evaluate whether the new furanone compounds are toxic to host cells, a cytotoxicity test was performed in three types of human cells: the monocytic cell line THP-1, human gingival fibroblasts (HGFs), and the human oral keratinocyte cell line HOK-16B. As

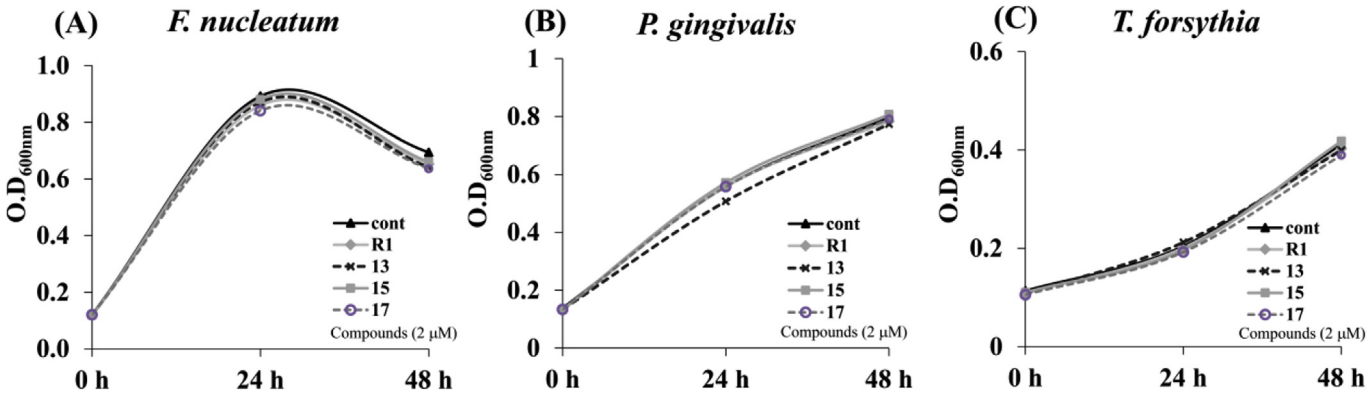

Fig. 4. Effects of furanone compounds on bacterial growth. (A) *F. nucleatum*, (B) *P. gingivalis*, and (C) *T. forsythia* were grown for 48 h under anaerobic conditions at 37 °C in the presence of the reference furanone compound (**R1**) or new furanone compounds (**13**, **15**, and **17**) at a concentration of 2 μM. Bacterial growth was monitored by measuring absorbance at 600 nm using a spectrophotometer.

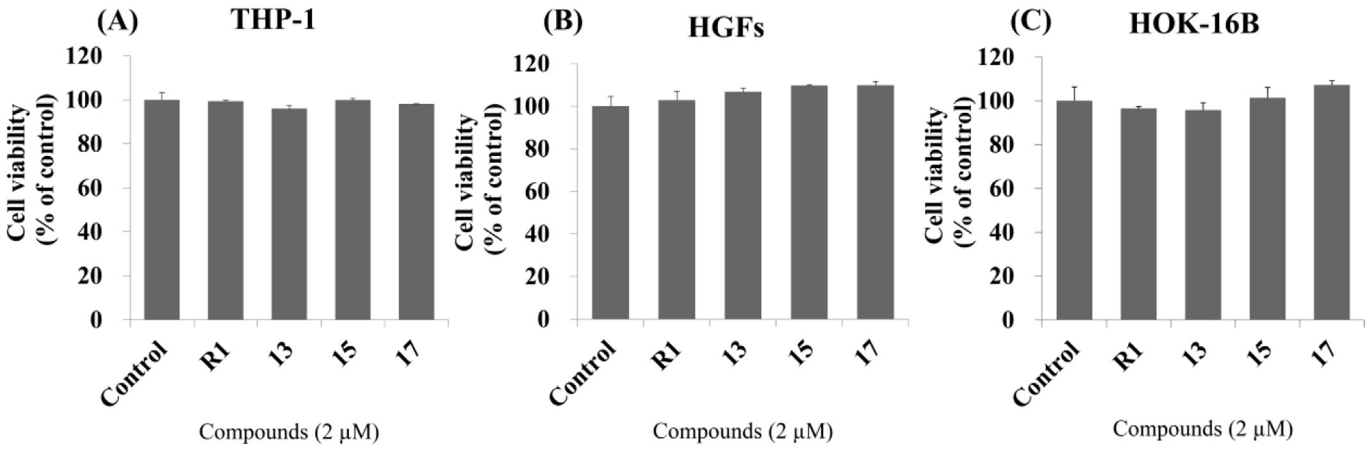

Fig. 5. Effects of furanone compounds on host cell viability. (A) THP-1 cells (1×10^5 cells/well), (B) HGFs (2×10^4 cells/well), and (C) HOK-16B cells (5×10^4 cells/well) cultured in 96-well plates were treated with the reference furanone compound (**R1**) and new furanone compounds (**13**, **15**, and **17**) for 24 h, and the cell viability was detected using Cell Counting Kit-8. The control was the non-treated group. The experiments were performed three times in triplicate and representative data are shown.

shown in Fig. 5, the compounds did not affect host cell viability at 2 μM.

2.2.5. Effect of furanone compounds on the host cell immune response

To confirm whether the new compounds induce an inflammatory response in host cells, the expression levels of proinflammatory cytokines, including interleukin (IL)-6 and IL-8, were analyzed by real-time reverse transcription-polymerase chain reaction (RT-PCR) after treating THP-1 cells and HGFs with the furanone compounds. Fig. 6 shows that the new furanone compounds (**13**, **15**, and **17**) did not induce an inflammatory response, whereas the reference compound **R1** or lipopolysaccharide (LPS; 1 μg/mL) significantly induced the gene expression of *IL-6* and *IL-8* in THP-1 cells (Fig. 6A and B). In HGFs, the new furanone compounds (**13**, **15**, and **17**) did not induce the gene expression of *IL-6* and *IL-8* (Fig. 6C and D), whereas the reference compound **R1** induced the gene expression of *IL-8*, and LPS (1 μg/mL) induced the gene expression of both cytokines.

3. Conclusion

We synthesized 3-(dibromomethylene)isobenzofuran-1(3H)-one derivatives and tested their inhibitory effects against the AI-2-mediated QS and biofilm formation of periodontopathogens. Our results demonstrate that bicyclic furanone derivatives containing a five-membered ring (**13**) or methylbenzene moieties (**15** and **17**) significantly inhibited the *F. nucleatum* AI-2 activity and biofilm formation of *F. nucleatum*, *P. gingivalis*, and *T. forsythia* without a bactericidal effect. The inhibitory activities of **13**, **15**, and **17** were similar to or better than that of the reference compound **R1**. Our new furanone compounds showed neither cytotoxicity nor induction of proinflammatory cytokine expression, whereas the reference compound **R1** showed cytotoxicity and induced the expression of proinflammatory cytokines such as IL-6 and IL-8 in human cells.

In addition, our results highlight the importance of the structural element of a bicyclic compound for its effective biofilm inhibition activity. First, compound **13,** which has a similar ring structure form to AI-2, showed good inhibition activity. Second, we found that the inhibitory activity was good when the compound had a short side chain. In particular, compound **17**, in which the methyl group was introduced at a similar position to that of the existing monocyclic brominated furanone, exhibited the highest inhibitory activity. As the widespread use of traditional antibacterial agents such as disinfectants and antibiotics can lead to the development of drug-resistant strains of bacteria and even kill beneficial bacteria, the new compounds **13**, **15**, and **17** can be good candidates for prevention of the biofilm formation of periodontopathogens. The effect of these compounds on other bacteria

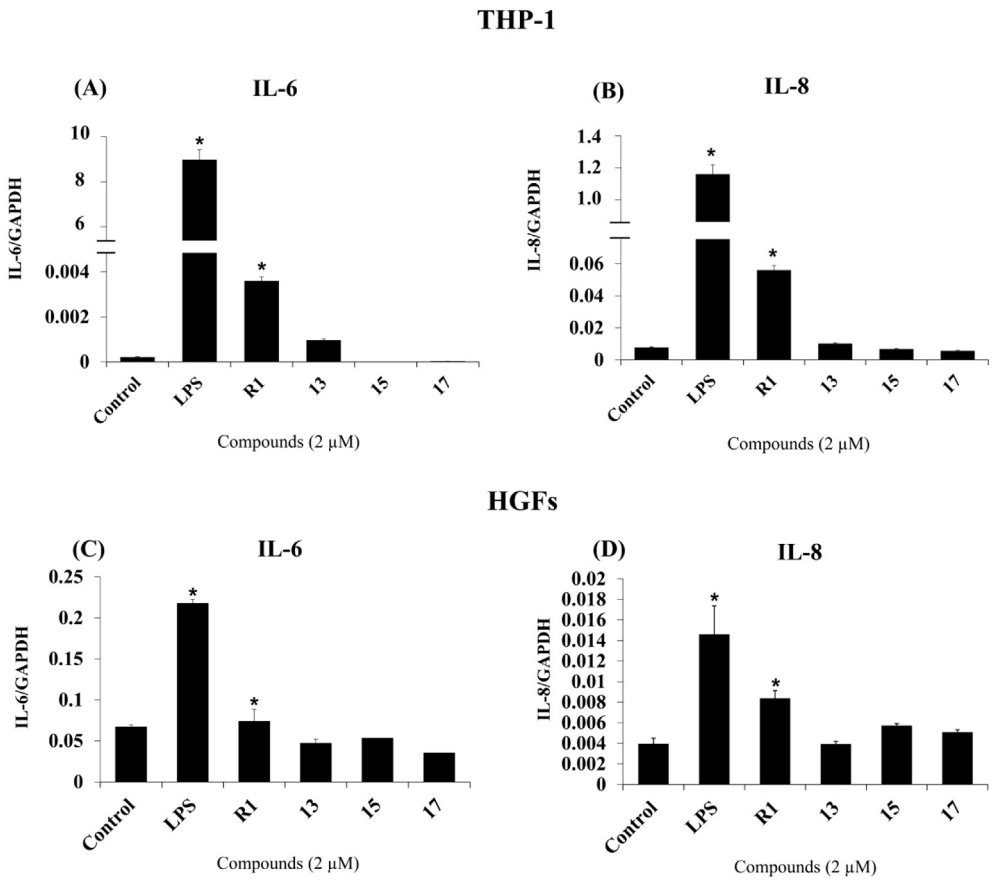

Fig. 6. Effects of furanone compounds on proinflammatory cytokines. THP-1 cells (1×10^6 cells/well, A and B) and HGFs (2×10^5 cells/well, C and D) cultured in 6-well plates were treated with the reference furanone compound (**R1**) and new furanone compounds (**13**, **15**, and **17**) for 24 h. The expression levels of *IL-6* and *IL-8* mRNA were analyzed by real-time RT-PCR. The experiments were performed three times in triplicate, and representative data are shown. $^*p < 0.05$ compared to the untreated control value.

involved in infectious diseases remains to be assessed.

4. Experimental part

4.1. Chemistry

The ^1H, ^{13}C NMR-spectra and heteronuclear multiple bond correlation (HMBC) were measured with an Agilent 400-MR DD2 Magnetic Resonance System (400 MHz) and a Varian/Oxford As-500 (500 MHz) spectrophotometer. Chemical shifts were measured as parts per million (δ values) from tetramethylsilane as an internal standard at probe temperature in $CDCl_3$ or DMSO-D_6 for neutral compounds. Coupling constants are provided in Hz, with the following spectral pattern designations: s, singlet; d, doublet; t, triplet; q, quartet; quint, quintet; m, multiplet; br, broad; app, apparent. Melting points were determined on an Electro-thermal IA 9100 apparatus without correction. Reactions that needed anhydrous conditions were carried out in flame-dried glassware under positive pressure of dry N_2 using standard Schlenk line techniques. Evaporation of solvents was performed at reduced pressure using a rotary evaporator. TLC was performed using silica gel 60F254 coated on aluminum sheet (E. Merck, Art.5554). Column chromatography was performed on silica gel (Merck. 7734 or 9385 Kiesel gel 60), and eluent was mentioned in each procedure. Elemental analyses were performed on a Thermo Scientific model Flash 2000 instrument (Waltham, MA, USA) and the results are within ±0.4% of the theoretical values. High resolution mass spectra (HRMS) were recorded on a ThermoFinnigan LCQ™ Classic, Quadrupole Ion-Trap Mass Spectrometer. HPLC analyses were carried out on an Agilent HP1100 system (Santa Clara, CA, USA), composed of an auto sampler, quaternary pump, photodiode array detector (DAD), and HP Chemstation software. The separation was carried out on a poroshell 120 EC-C18 column 4.6 × 50 mm i.d. (2.7 μm particle size) with 0.1% TFA in water (A) and acetonitrile (B) as a mobile phase at a flow rate of 1 mL/min at 20 °C. Method: 100% A and 0% B (0 min), 50% A and 50% B (5 min), 5% A and 95% B (15 min), 5% A and 95% B (22 min), 100% A and 0% B (23 min), 100% A and 0% B (25 min). Details are given below for one example of each reaction type; the syntheses and characterization of analogs are reported in the Supplementary Information. All materials were obtained from commercial supplier and used without further purification unless otherwise noted.

4.1.1. General procedure for the preparation of 3 or 4-alkoxyphthalic anhydride (**7a**–**7d, 9a**–**9d**)

Following a reported procedure [34], we added H_2SO_4 (0.054 mL, 1.02 mmol) to a stirred solution of 3- or 4-hydroxyphthalic acid (1.09 g, 6.00 mmol) in 12 mL of MeOH and the reaction was stirred at reflux overnight. Solvent was removed under reduced pressure and the solid residue obtained was dissolved in dichloromethane (40 mL) and washed with water (20 × 3 mL). The combined organic layer was dried over anhydr $MgSO_4$, filtered and concentrated under reduced pressure to provide crude dimethyl 4-hydroxyphthalate. The crude dimethyl 3- or 4-hydroxyphthalate was dissolved in 3 mL of acetone and K_2CO_3 (1.3 g, 9.5 mmol) was added to the solution. The mixture was stirred

at room temperature for 1 h. Alkyl iodide (5.7 mmol) was added, and the mixture was stirred at reflux overnight. K_2CO_3 was removed by filtration and the solvent was removed under reduced pressure to provide dimethyl 3- or 4-alkoxyphthalate.

A solution of dimethyl 3- or 4-alkoxyphthalate in 3 mL of acetone was treated with an aq solution of NaOH (0.34 g, 8.4 mmol) in 2 mL water and then the resulting solution was stirred at room temperature overnight. After evaporation of the solvent, the mixture was acidified with 6 M HCl to pH 2 and concentrated under reduced pressure. Then, the 3- or 4-alkoxyphthalic acid was dissolved in 4 mL of Ac_2O and the solution was heated at reflux for 18 h. Upon cooling to room temperature, the resulting solution was concentrated by rotary evaporation and then the residue was purified with flash column chromatography. The desired products **7a-7d** and **9a**–**9d** were obtained.

*4.1.1.1. 4-Ethoxyphthalic anhydride (**7a**).* Yield 0.83 g (72%). ^{1}H NMR (DMSO-d_6, 500 MHz) δ 7.96 (d, J = 8.4 Hz, 1H), 7.53 (d, J = 2.3 Hz, 1H), 7.45 (dd, J = 8.4, 2.3 Hz, 1H), 4.25 (q, J = 7.0 Hz, 2H), 1.37 (t, J = 7.0 Hz, 3H). ^{13}C NMR (DMSO-d_6, 125 MHz) δ 164.92, 163.1, 162.6, 134.0, 127.2, 123.1, 122.5, 109.6, 64.9, 14.3.

*4.1.1.2. 4-Propoxyphthalic anhydride (**7b**).* Yield 0.86 g (70%). ^{1}H NMR (DMSO-d_6, 500 MHz) δ 7.97 (d, J = 8.4 Hz, 1H), 7.55 (d, J = 2.2 Hz, 1H), 7.47 (dd, J = 8.4, 2.3 Hz, 1H), 4.16 (t, J = 6.5 Hz, 2H), 1.81–1.72 (m, 2H), 0.99 (t, J = 7.4 Hz, 3H). 13C NMR (DMSO-d_6, 125 MHz) δ 165.1, 163.1, 162.7, 134.0, 127.2, 123.1, 122.5, 109.6, 70.5, 21.7, 10.2.

*4.1.1.3. 4-Butoxyphthalic anhydride (**7c**).* Yield 0.97 g (74%). ^{1}H NMR (DMSO-d_6, 500 MHz) δ 7.97 (d, J = 8.4 Hz, 1H), 7.56 (d, J = 2.3 Hz, 1H), 7.47 (dd, J = 8.5, 2.2 Hz, 1H), 4.20 (t, J = 6.5 Hz, 2H), 1.79–1.68 (m, 2H), 1.51–1.38 (m, 2H), 0.94 (t, J = 7.4 Hz, 3H). 13C NMR (DMSO-d_6, 125 MHz) δ 165.1, 163.1, 162.7, 134.0, 127.2, 123.2, 122.5, 109.6, 68.8, 30.3, 18.6, 13.6.

*4.1.1.4. 4-Pentyloxyphthalic anhydride (**7d**).* Yield 0.98 g (70%). ^{1}H NMR (DMSO-d_6, 500 MHz) δ 7.96 (d, J = 8.4 Hz, 1H), 7.55 (d, J = 2.2 Hz, 1H), 7.46 (dd, J = 8.4, 1.8 Hz, 1H), 4.19 (t, J = 6.5 Hz, 2H), 1.82–1.69 (m, 2H), 1.47–1.28 (m, 4H), 0.90 (t, J = 7.1 Hz, 3H).

*4.1.1.5. 3-Ethoxyphthalic anhydride (**9a**).* Yield 0.61 g (53%). ^{1}H NMR (DMSO-d_6, 500 MHz) δ 7.92 (dd, J = 8.5, 7.4 Hz, 1H), 7.58 (dd, J = 16.4, 7.9 Hz, 2H), 4.31 (q, J = 7.0 Hz, 2H), 1.40 (t, J = 7.0 Hz, 3H). ^{13}C NMR (DMSO-d_6, 125 MHz) δ 163.2, 160.6, 156.9, 138.7, 133.0, 120.2, 116.8, 116.4, 65.0, 14.3.

*4.1.1.6. 3-Propoxyphthalic anhydride (**9b**).* Yield 0.58 g (47%). ^{1}H NMR (DMSO-d_6, 500 MHz) δ 7.92 (dd, J = 8.4, 7.4 Hz, 1H), 7.60 (d, J = 8.5 Hz, 1H), 7.56 (d, J = 7.4 Hz, 1H), 4.20 (t, J = 6.4 Hz, 2H), 1.85–1.75 (m, 2H), 1.02 (t, J = 7.4 Hz, 3H). ^{13}C NMR (DMSO-d_6, 125 MHz) δ 163.2, 160.6, 157.1, 138.7, 133.0, 120.3, 116.8, 116.4, 70.5, 21.7, 10.1.

*4.1.1.7. 3-Butoxyphthalic anhydride (**9c**).* Yield 0.59 g (45%). ^{1}H NMR (DMSO-d_6, 500 MHz) δ 7.91 (dd, J = 8.4, 7.4 Hz, 1H), 7.60 (d, J = 8.5 Hz, 1H), 7.56 (d, J = 7.3 Hz, 1H), 4.24 (t, J = 6.4 Hz, 2H), 1.82–1.71 (m, 2H), 1.54–1.42 (m, 2H), 0.95 (t, J = 7.4 Hz, 3H). ^{13}C NMR (DMSO-d_6, 125 MHz) δ 163.2, 160.5, 157.1, 138.7, 133.0, 120.2, 116.8, 116.4, 68.8, 30.3, 18.5, 13.6.

*4.1.1.8. 3-Pentyloxyphthalic anhydride (**9d**).* Yield 0.64 g (46%). ^{1}H NMR (DMSO-d_6, 500 MHz) δ 7.91 (dd, J = 8.4, 7.4 Hz, 1H), 7.60 (d, J = 8.5 Hz, 1H), 7.55 (d, J = 7.4 Hz, 1H), 4.23 (t, J = 6.5 Hz, 2H), 1.79 (dd, J = 14.1, 7.3 Hz, 2H), 1.52–1.30 (m, 4H), 0.90 (t, J = 7.2 Hz, 3H). ^{13}C NMR (DMSO-d_6, 125 MHz) δ 163.2, 160.5, 157.1, 138.7, 133.0, 120.2, 116.8, 116.4, 69.1, 28.0, 27.4, 21.8, 13.9.

*4.1.2. General procedure for the preparation of bicyclic brominated furanone derivatives (**10**–**18d**)*

Triphenylphosphine (1.60 g, 6.00 mmol) was dissolved in 6 mL of THF and the solution was cooled to 0 °C under N_2. A solution of CBr_4 (1.00 g, 3.00 mmol) in THF (1.00 mL per mmol PPh_3) was added to the THF (6 mL) solution of PPh_3 and the reaction was stirred until the color changed to yellow. Triethylamine (TEA) (1.1 mL, 6.0 mmol) was added dropwise to the mixture over 5 min, after which a solution of an anhydride compound (**1**–**9d**, 1.00 mmol) in THF (1.0 mL per mmol phthalic anhydride) was incrementally added. The reaction was stirred for 1 h at 0 °C, after which it was allowed to warm to room temperature and stirred overnight. The reaction was quenched by addition of sat aq NH_4Cl solution (30 mL). The phases were then separated, and the crude product was extracted with hexane from the aqueous layer (30 × 3 mL). The combined organic layers were concentrated under reduced pressure. The residue was dissolved in Et_2O (25 mL) and filtered over a Celite pad (7.0 × 3.0 cm). The resulting filtrate was concentrated by rotary evaporation and the crude products were purified through the use of silica gel column chromatography (5–15% EtOAc in hexane). The desired products were obtained.

*4.1.2.1. 3-(Dibromomethylene)isobenzofuran-1(3H)-one (**10**).* White solid, yield 0.091 g (30%). m.p. 136–138 °C; ^{1}H NMR (DMSO-d_6, 500 MHz) δ 8.32 (d, J = 8.0 Hz, 1H, H-4), 7.95 (d, J = 7.6 Hz, 1H, H-7), 7.90 (t, J = 7.7 Hz, 1H, H-5), 7.75 (t, J = 7.5 Hz, 1H, H-6); ^{13}C NMR (DMSO-d_6,125 MHz) δ 164.0 (C-1), 145.5 (C-3), 135.8 (C-3a), 135.6 (C-5), 131.4 (C-6), 126.0 (C-7), 125.3 (C-7a), 123.7 (C-4), 77.3 (=CBr_2). Anal. Calcd. for $C_9H_4Br_2O_2$: C, 35.57; H, 1.33. Found: C, 35.62; H, 1.34. HRMS (ESI) *m/z*: Anal. calcd. for [M+Na]+ $C_9H_4Br_2NaO_2$+: 324.8470; found 324.8471. HPLC purity: 99.9%.

*4.1.2.2. 3-(Dibromomethylene)hexahydroisobenzofuran-1(3H)-one (**11**).* Colorless oil, yield 0.12 g (40%). ^{1}H NMR ($CDCl_3$, 500 MHz) δ 3.31–3.19 (m, 1H), 2.98 (t, J = 6.8 Hz, 1H), 2.22 (t, J = 14.3 Hz, 2H), 1.72 (d, J = 15.0 Hz, 2H), 1.35–1.05 (m, 4H). ^{13}C NMR ($CDCl_3$, 125 MHz) δ 174.1, 158.2, 68.9, 40.7, 40.0, 26.5, 23.0, 22.3. Anal. Calcd. for $C_9H_{10}Br_2O_2$: C, 34.87; H, 3.25. Found: C, 34.89; H, 3.24. HRMS (ESI) *m/z*: Anal. calcd. for [M+Na]+ $C_9H_{10}Br_2NaO_2$+: 330.8940; found 330.8942. HPLC purity: 97.8%.

*4.1.2.3. 3-(Dibromomethylene)-4,5,6,7-tetrahydroisobenzofuran-1(3H)-one (**12**).* White solid, yield 0.20 g (65%). m.p. 128–130 °C; ^{1}H NMR (DMSO-d_6, 500 MHz) δ 2.74–2.69 (m, 2H), 2.16–2.11 (m, 2H), 1.72–1.68 (m, 2H), 1.63–1.59 (m, 2H). ^{13}C NMR (DMSO-d_6, 125 MHz) δ 166.5, 149.7, 148.6, 131.2, 78.4, 25.0, 21.3, 20.5, 20.1. Anal. Calcd. for $C_9H_8Br_2O_2$: C, 35.10; H, 2.62. Found: C, 35.19; H, 2.60. HRMS (ESI) *m/z*: Anal. calcd. for [M+Na]+ $C_9H_8Br_2NaO_2$+: 328.8783; found 328.8786. HPLC purity: 99.0%.

*4.1.2.4. 3-(Dibromomethylene)hexahydro-1H-cyclopenta[c]furan-1-one (**13**).* Yellowish oil, yield 0.071 g (24%). ^{1}H NMR (DMSO-d_6, 500 MHz) δ 3.50–3.48 (m, 2H), 2.04–1.82 (m, 4H), 1.73–1.66 (m, 1H), 1.39–1.30 (m, 1H). ^{13}C NMR (DMSO-d_6, 125 MHz) δ 176.5, 155.4, 68.0, 45.8, 43.8, 32.2, 30.8, 25.6. Anal. Calcd. for $C_8H_8Br_2O_2$: C, 32.47; H, 2.72. Found: C, 32.50; H, 2.80. HRMS (ESI) *m/z*: Anal. calcd. for [M+Na]+ $C_8H_8Br_2NaO_2$+: 316.8783; found 316.8780. HPLC purity: 99.5%.

*4.1.2.5. 3-(Dibromomethylene)-3,4,5,6-tetrahydro-1H-cyclopenta[c]furan-1-one (**14**).* Brown solid, yield 0.080 g (27%). m.p. 120–122 °C; ^{1}H NMR (DMSO-d_6, 500 MHz) δ 2.96–2.91 (m, 2H),

2.48–2.39 (m, 4H). ^{13}C NMR (DMSO-d_6, 125 MHz) δ 162.5, 162.2, 146.5, 140.9, 79.4, 29.5, 28.1, 25.1. Anal. Calcd. for $C_8H_6Br_2O_2$: C, 32.69; H, 2.06. Found: C, 32.71; H, 2.06. HRMS (ESI) *m/z*: Anal. calcd. for [M+Na]+ $C_8H_6Br_2NaO_2$+: 314.8627; found 314.8625. HPLC purity: 97.3%.

*4.1.2.6. 3-(Dibromomethylene)-5-methylisobenzofuran-1(3H)-one (**15**).* White solid, yield 0.076 g (24%). m.p. 128–130 °C; ^{1}H NMR (DMSO-d_6, 500 MHz) δ 8.18 (s, 1H, H-4), 7.87 (d, J = 7.9 Hz, 1H, H-7), 7.60 (d, J = 7.8 Hz, 1H, H-6), 2.52 (s, 3H, -CH_3). ^{13}C NMR (DMSO-d_6, 125 MHz) δ 164.0 (C-1), 146.9 (C-5), 145.5 (C-3), 136.3 (C-3a), 132.6 (C-6), 126.0 (C-7), 124.0 (C-4), 122.9 (C-7a), 77.0 (=CBr_2), 22.0 (-CH_3). Anal. Calcd. for $C_{10}H_6Br_2O_2$: C, 37.77; H, 1.90. Found: C, 37.78; H, 2.03. HRMS (ESI) *m/z*: Anal. calcd. for [M+Na]+ $C_{10}H_6Br_2NaO_2$+: 338.8627; found 338.8629. HPLC purity: 98.9%.

*4.1.2.7. 3-(Dibromomethylene)-5-ethoxyisobenzofuran-1(3H)-one (**16a**).* White solid, yield 0.70 g (20%). m.p. 156–158 °C; ^{1}H NMR (DMSO-d_6, 500 MHz) δ 7.90 (d, J = 8.5 Hz, 1H, H-7), 7.76 (s, 1H, H-4), 7.31 (d, J = 7.0 Hz, 1H, H-6), 4.20 (q, J = 6.8 Hz, 2H, -OCH_2), 1.39 (t, J = 6.9 Hz, 3H, -CH_3). ^{13}C NMR (DMSO-d_6, 125 MHz) δ 164.3 (C-5), 163.6 (C-1), 145.2 (C-3), 138.2 (C-3a), 128.0 (C-7), 118.4 (C-6), 117.3 (C-7a), 108.7 (C-4), 77.4 (=CBr_2), 64.6 (-OCH_2), 14.3 (-CH_3). Anal. Calcd. for $C_{11}H_8Br_2O_3$: C, 37.97; H, 2.32. Found: C, 37.97; H, 2.39. HRMS (ESI) *m/z*: Anal. calcd. for [M+Na]+ $C_{11}H_8Br_2NaO_3$+: 368.8732; found 368.8731. HPLC purity: > 99.9%.

*4.1.2.8. 3-(Dibromomethylene)-5-propoxyisobenzofuran-1(3H)-one (**16b**).* White solid, yield 0.69 g (19%). m.p. 121–123 °C; ^{1}H NMR (DMSO-d_6, 500 MHz) δ 7.89 (d, J = 8.5 Hz, 1H, H-7), 7.75 (s, 1H, H-4), 7.31 (d, J = 8.5 Hz, 1H, H-6), 4.09 (t, J = 6.4 Hz, 2H, -OCH_2), 1.84–1.75 (m, 2H, -CH_2), 1.00 (t, J = 7.4 Hz, 3H, -CH_3). ^{13}C NMR (DMSO-d_6, 125 MHz) δ 164.4 (C-5), 163.5 (C-1), 145.1 (C-3), 138.1 (C-3a), 127.9 (C-7), 118.5 (C-6), 117.3 (C-7a), 108.7 (C-4), 77.4 (=CBr_2), 70.2 (-OCH_2), 21.8(-CH_2), 10.3(-CH_3). Anal. Calcd. for $C_{12}H_{10}Br_2O_3$: C, 39.81; H, 2.78. Found: C, 39.85; H, 2.88. HRMS (ESI) *m/z*: Anal. calcd. for [M+Na]+ $C_{12}H_{10}Br_2NaO_3$+: 382.8889; found 382.8887. HPLC purity: 97.6%.

*4.1.2.9. 3-(Dibromomethylene)-5-butoxyisobenzofuran-1(3H)-one (**16c**).* White solid, yield 0.79 g (21%). m.p. 127–129 °C; ^{1}H NMR (DMSO-d_6, 500 MHz) δ 7.90 (d, J = 8.5 Hz, 1H, H-7), 7.76 (s, 1H, H-4), 7.31 (d, J = 8.5 Hz, 1H, H-6), 4.14 (t, J = 6.4 Hz, 2H, -OCH_2), 1.80–1.68 (m, 2H, -CH_2), 1.50–1.39 (m, 2H, -CH_2), 0.94 (t, J = 7.4 Hz, 3H, -CH_3). ^{13}C NMR (DMSO-d_6, 125 MHz) δ 164.4 (C-5), 163.5 (C-1), 145.2 (C-3), 138.2 (C-3a), 128.0 (C-7), 118.4 (C-6), 117.3 (C-7a), 108.7 (C-4), 77.4 (=CBr_2), 68.4 (-OCH_2), 39.5 (-CH_2), 30.4 (-CH_2), 18.6 (-CH_2), 13.6 (-CH_3). Anal. Calcd. for $C_{13}H_{12}Br_2O_3$: C, 41.52; H, 3.22. Found: C, 41.62; H, 3.32. HRMS (ESI) *m/z*: Anal. calcd. for [M+Na]+ $C_{13}H_{12}Br_2NaO_3$+: 396.9045; found 396.9047. HPLC purity: 98.6%.

*4.1.2.10. 3-(Dibromomethylene)-5-(pentyloxy)isobenzofuran-1(3H)-one (**16d**).* White solid, yield 0.74 g (19%). m.p. 100–102 °C; ^{1}H NMR (DMSO-d_6, 500 MHz) δ 7.88 (d, J = 8.5 Hz, 1H, H-7), 7.74 (s, 1H, H-4), 7.30 (d, J = 8.6 Hz, 1H, H-6), 4.12 (t, J = 6.4 Hz, 2H, -OCH_2), 1.81–1.72 (m, 2H, -CH_2), 1.46–1.29 (m, 4H, -CH_2), 0.90 (t, J = 7.1 Hz, 3H, -CH_3). ^{13}C NMR (DMSO-d_6, 125 MHz) δ 164.4 (C-5), 163.5 (C-1), 145.1 (C-3), 138.1 (C-3a), 127.9 (C-7), 118.4 (C-6), 117.3 (C-7a), 108.7 (C-4), 77.4 (=CBr_2), 68.7 (-CH_2), 28.1 (-CH_2), 27.5 (-CH_2), 21.8 (-CH_2), 13.9(-CH_3). Anal. Calcd. for $C_{14}H_{14}Br_2O_3$: C, 43.11; H, 3.62. Found: C, 43.18; H, 3.70. HRMS (ESI) *m/z*: Anal. calcd. for [M+Na]+ $C_{14}H_{14}Br_2NaO_3$+: 410.9202; found 410.9203. HPLC purity: 99.2%.

*4.1.2.11. 3-(Dibromomethylene)-7-methylisobenzofuran-1(3H)-one (**17**).* White solid, yield 0.83 g (26%). m.p. 138–140 °C; ^{1}H NMR (DMSO-d_6, 500 MHz) δ 8.18 (d, J = 7.9 Hz, 1H, H-4), 7.77 (t, J = 7.7 Hz, 1H, H-5), 7.55 (d, J = 7.5 Hz, 1H, H-6), 2.61 (s, 3H). ^{13}C NMR (DMSO-d_6, 125 MHz) δ 164.0 (C-1), 145.2 (C-3), 139.8 (C-7), 136.1 (C-3a), 135.2 (C-5), 132.9 (C-6), 122.8 (C-7a), 121.3 (C-4), 76.5 (=CBr_2), 16.9 (-CH_3). Anal. Calcd. for $C_{10}H_6Br_2O_2$: C, 37.77; H, 1.90. Found: C, 37.78; H, 1.86. HRMS (ESI) *m/z*: Anal. calcd. for [M+Na]+ $C_{10}H_6Br_2NaO_2$+: 338.8627; found 338.8628. HPLC purity: 99.8%.

*4.1.2.12. 3-(Dibromomethylene)-7-ethoxyisobenzofuran-1(3H)-one (**18a**).* White solid, yield 0.66 g (19%). m.p. 141–143 °C; ^{1}H NMR (DMSO-d_6, 500 MHz) δ 7.87 (d, J = 7.8 Hz, 1H, H-4), 7.82 (t, J = 8.0 Hz, 1H, H-5), 7.32 (d, J = 8.2 Hz, 1H, H-6), 4.24 (q, J = 6.9 Hz, 2H, -OCH_2), 1.38 (t, J = 7.0 Hz, 3H, -CH_3). ^{13}C NMR (DMSO-d_6, 125 MHz) δ 161.4 (C-1), 157.8 (C-7), 145.1 (C-3), 137.8 (C-5), 137.7 (C-3a), 115.3 (C-4), 114.7 (C-6), 111.8 (C-7a), 76.7 (=CBr_2), 64.6 (-OCH_2), 14.3 (-CH_3). Anal. Calcd. for $C_{11}H_8Br_2O_3$: C, 37.97; H, 2.32. Found: C, 37.91; H, 2.42. HRMS (ESI) *m/z*: Anal. calcd. for [M+Na]+ $C_{11}H_8Br_2NaO_3$+: 368.8732; found 368.8733. HPLC purity: 99.8%.

*4.1.2.13. 3-(Dibromomethylene)-7-propoxyisobenzofuran-1(3H)-one (**18b**).* White solid, yield 0.65 g (18%). m.p. 101–103 °C; ^{1}H NMR (DMSO-d_6, 500 MHz) δ 7.87 (d, J = 7.8 Hz, 1H, H-4), 7.82 (t, J = 8.0 Hz, 1H, H-5), 7.32 (d, J = 8.3 Hz, 1H, H-6), 4.13 (t, J = 6.4 Hz, 2H, -OCH_2), 1.85–1.73 (m, 2H, -CH_2), 1.01 (t, J = 7.4 Hz, 3H, -CH_3). ^{13}C NMR (DMSO-d_6, 125 MHz) δ 161.4 (C-1), 157.9 (C-7), 145.1 (C-3), 137.8 (C-5), 137.7 (C-3a), 115.4 (C-4), 114.8 (C-6), 111.9 (C-7a), 76.7 (=CBr_2), 70.1 (-OCH_2), 21.8 (-CH_2), 10.2 (-CH_3). Anal. Calcd. for $C_{12}H_{10}Br_2O_3$: C, 39.81; H, 2.78. Found: C, 39.79; H, 2.78. HRMS (ESI) *m/z*: Anal. calcd. for [M+Na]+ $C_{12}H_{10}Br_2NaO_3$+: 382.8889; found 382.8891. HPLC purity: 96.2%.

*4.1.2.14. 3-(Dibromomethylene)- 7-butoxyisobenzofuran-1(3H)-one (**18c**).* White solid, yield 0.68 g (18%). m.p. 86–88 °C; ^{1}H NMR (DMSO-d_6, 500 MHz) δ 7.88 (d, J = 7.8 Hz, 1H, H-4), 7.82 (t, J = 8.0 Hz, 1H, H-5), 7.33 (d, J = 8.3 Hz, 1H, H-6), 4.18 (t, J = 6.4 Hz, 2H, -OCH_2), 1.80–1.66 (m, 2H, -CH_2), 1.53–1.37 (m, 2H, -CH_2), 0.94 (t, J = 7.4 Hz, 3H, -CH_3). ^{13}C NMR (DMSO-d_6, 125 MHz) δ 161.4 (C-1), 157.9 (C-7), 145.1 (C-3), 137.9 (C-5), 137.7 (C-3a), 115.4 (C-4), 114.8 (C-6), 111.9 (C-7a), 76.7 (=CBr_2), 68.5 (-CH_2), 30.4 (-CH_2), 18.6 (-CH_2), 13.7 (-CH_3). Anal. Calcd. for $C_{13}H_{12}Br_2O_3$: C, 41.52; H, 3.22. Found: C, 41.57; H, 3.23. HRMS (ESI) *m/z*: Anal. calcd. for [M+Na]+ $C_{13}H_{12}Br_2NaO_3$+: 396.9045; found 396.9047. HPLC purity: 97.7%.

*4.1.2.15. 3-(Dibromomethylene)-7-(pentyloxy)isobenzofuran-1(3H)-one (**18d**).* White solid, yield 0.62 g (16%). m.p. 72–74 °C; ^{1}H NMR (DMSO-d_6, 500 MHz) δ 7.89 (d, J = 7.8 Hz, 1H, H-4), 7.83 (t, J = 8.0 Hz, 1H, H-5), 7.34 (d, J = 8.3 Hz, 1H, H-6), 4.18 (t, J = 6.5 Hz, 2H, -OCH_2), 1.84–1.70 (m, 2H, -CH_2), 1.50–1.28 (m, 4H, -CH_2CH_2), 0.89 (t, J = 7.2 Hz, 3H, -CH_3). ^{13}C NMR (DMSO-d_6, 125 MHz) δ 161.4 (C-1), 157.9 (C-7), 145.1 (C-3), 137.9 (C-5), 137.7 (C-3a), 115.4 (C-4), 114.8 (C-6), 111.9 (C-7a), 76.6 (=CBr_2), 68.8 (-CH_2), 28.0 (-CH_2), 27.5 (-CH_2), 21.8 (-CH_2), 13.9 (-CH_3). Anal. Calcd. for $C_{14}H_{14}Br_2O_3$: C, 43.11; H, 3.62. Found: C, 43.14; H, 3.62. HRMS (ESI) *m/z*: Anal. calcd. for [M+Na]+ $C_{14}H_{14}Br_2NaO_3$+: 410.9202; found 410.9201. HPLC purity: 99.2%.

4.2. Biological assay

4.2.1. Bacteria culture

AI-2 reporter strain, *Vibrio harveyi* BB170 (ATCC BAA-1117) was cultured aerobically at 30 °C in autoinducer bioassay (AB) medium consisting of 0.30 M sodium chloride, 0.050 M magnesium sulfate, 0.2% casamino acids, 10 mM potassium phosphate (pH 7.0), 1.0 mM L-arginine and 2% glycerol with shaking. *F. nucleatum* (ATCC 25586) and *P. gingivalis* (ATCC 33277) were cultured anaerobically (10% H_2,

10% CO_2, 80% N_2) in brain heart infusion broth supplemented with vitamin K (0.2 mg/mL) and hemin (10 mg/mL) at 37 °C. *T. forsythia* (ATCC 43037) was cultured anaerobically in new oral spirochete (NOS) broth (ATCC medium 1494) supplemented with *N*-acetylmuramic acid (0.01 μg/mL) and vitamin K (0.2 mg/mL) at 37 °C.

4.2.2. Purification of AI-2

AI-2 of F. nucleatum was partially purified as described previously [20]. In brief, F. nucleatum which was cultured overnight was diluted 1:20 with fresh culture medium. After incubating the culture mixture until the late logarithmic phase (OD660 nm = 0.7), the culture supernatants were collected by centrifugation at 10,000×*g* at 4 °C. The culture supernatants were passed through 0.2 μm pore-size membrane filters (Sartorius Stedium Biotech, Goettingen, Germany) and the filtrates were subsequently passed through a Centricon YM-3 3-kDa exclusion filter (Millipore, Bedford, MA). Then the filtrates were chromatographed on a C18 Sep-Pak reverse-phase column (Waters Co., Milford, MA) according to the manufacturer's instructions.

4.2.3. AI-2 activity test

As QS molecules stimulates the luciferase operon (lux gene) to express luciferase of *V. harveyi* BB170, bioluminescence of V. harveyi BB170 was determined as AI-2 activity. *V. harveyi* BB170 was diluted to a concentration of 1×10^6 bacteria/ml in fresh AB medium. Then the bacterial suspension was mixed with 10% (vol/vol) of partially purified AI-2 of *F. nucleatum* in the presence or absence of the furanone compounds (the reference compound **R1** and new synthesized furanone analogs) of various concentrations, and incubated for 1–6 h at 30 °C under aerobic condition with shaking. The reference compound **R1** was (5Z)-4-bromo-5-(bromomethylene)-2(5H)-furanone. The bioluminescence was measured using a luminometer (GloMax-Multi detection system, Promega, Madison, WI, USA) and the value was converted into a percentage out of untreated control value.

4.2.4. Biofilm formation assay

Biofilm formation assay was performed by crystal violet staining and confocal laser scanning microscopy. Bacterial suspensions were added to 24-well plates with round glass slips (12 mm radius) in the presence of F. nucleatum AI-2 (10% vol/vol) and the furanone compounds (the reference furanone compound and new synthesized furanone analogs)at various concentrations. The initial number of F. nucleatum, P. gingivalis, and T. forsythia was 2 × 107 bacteria/mL, 2 × 108 bacteria/mL, and 2 × 108 bacteria/mL, respectively and incubated for 48 h under anaerobic condition (10% H_2, 10% CO_2, 80% N_2). After 48 h, biofilms formed on the glass slips were washed with phosphate buffered saline three times and stained with 1% crystal violet for 10 min and destained with 1 mL of acetone–alcohol (20:80, vol/vol). The absorbance at 595 nm of the destaining solution containing crystal violet was measured using a microplate reader (Wallac Victor3 microtiter, PerkinElmer Life Sciences, Waltham, MA).

Biofilm which was formed on the glass slips was stained by the Live/Dead-BacLight bacterial viability kit (Invitrogen, Grand Island, NY) and then observed using a confocal scanning laser microscope (Carl Zeiss LSM 700, Germany) at a magnification of 1000× and quantified by measuring fluorescence intensity and average thickness of the biofilm using Carl Zeiss LSM 700 program. Biomass was determined by dividing total intensity by the area where the fluorescence was obtained.

4.2.5. Planktonic bacterial growth test

F. nucleatum, P. gingivalis, and *T. forsythia* were grown anaerobically at 37 °C in the presence or absence of the furanone compounds (the reference furanone compound and new synthesized furanone analogs) without addition of *F. nucleatum* AI-2. *V. harveyi* BB170 was incubated aerobically at 30 °C in the presence or absence of the QSIs without addition of AI-2. Bacterial growth was monitored by measuring absorbance at 600 nm using a spectrophotometer.

4.2.6. Cytotoxicity test

Human monocytic cell line (THP-1), human gingival fibroblasts (HGFs) and Human oral keratinocyte cell line (HOK-16B) were used to evaluate the cytotoxicity of the compounds on host cells. THP-1 cells were cultured in RPMI 1640 media (Hyclone, Waltham, MA, USA) supplemented with 10% fetal bovine serum (Hyclone, Waltham, MA, USA), 2.05 mM L-glutamate and antibiotics (100 units/mL penicillin, 100 μg/mL streptomycin). HGFs were cultured in DMEM media (Hyclone, Waltham, MA, USA) supplemented with 4.0 mM L-glutamine, 4500 mg/L Glucose, sodium pyruvate, antibiotics (100 units/mL penicillin, 100 μg/mL streptomycin) and 10% fetal bovine serum. HOK-16B cells were cultured in Keratinocyte Basal Medium (Lonza, Walkersville, MD, USA) supplemented with insulin, epidermal growth factor, bovine pituitary extract, hydrocortisone and gentamicin sulfate amphotericin. Cultured THP-1 cells (1×10^5 cells/well) were seeded in 96 well microtiter plate and incubated in the presence of the compounds for 24 h. HGFs (2×10^4 cells/well) and HOK-16B (5×10^4 cells/well) were seeded in 96 well plates and grown until the confluence of 85%. The cells were then treated with the compounds and incubated for 24 h. The cell viability was evaluated using the Cell Counting Kit-8 (CCK-8, DOJINDO, Kumamoto, Japan) according to the manufacturer's protocol.

4.2.7. Evaluation the effect on host immune response

Effects of the compounds on host immune response was evaluated using real-time PCR. THP-1 cells (1×10^6 cells/well) and HGFs (2×10^5 cells/well) in 6 well plates were incubated at 37 °C for 24 h in the presence or absence of the compounds or lipopolysaccharides (LPS, 1 μg/mL) known as endotoxin of gram-negative bacteria that elicits strong immune responses in host cells. After 24 h incubation, RNA from THP-1 cell and HGFs cells was extracted using Easy-Blue total RNA extraction kit (iNtRON Biotechnology, Seongnam, Korea) according to the manufacturer's protocol. cDNA samples (2 μL) synthesized from the extracted RNA (1 μg) using a M-MLV Reverse Transcription kit (Promega, Madison, WI) were mixed with each primer pairs (10 pM) and Power SYBR Green Master Mix (Applied Biosystems, Warrington, UK) in a 20 μl reaction volume. The mixtures were subjected to ABI PRISM 7500 Fast Real-Time PCR system (Applied Biosystems, Foster City, CA, USA) using the following thermocycling: amplification for 40 cycles composed of a denaturation step at 95 °C for 15 s, an annealing and extension step at 60 °C for 1 min. Glyceraldehyde 3-phosphate dehydrogenase (GAPDH) gene, the housekeeping gene, was used as a reference gene for normalization of gene expression level of inflammatory cytokines including interleukin 6 (IL-6) and interleukin 8 (IL-8). The sequences of the primers used in this study were as follows: 5′-GTG GCC AGC CGA GCC-3′ and 5′-TGA AGG GGT TGA TGG CA-3′ for GAPDH; 5′-GAT TCA ATG AGG AGA CTT GCC TGG-3′, 5′-GCA GAA CTG GAT CAG GAC TTT-3′ for IL-6; 5′-CTG TGT GAA GGT GCA GTT TTG C-3′ and 5′- AAC TTC TCC ACA ACC CTC TGC-3′ for IL-8.

4.2.8. Statistical analysis

Statistical analysis was performed using Student's *t*-test. Statistically significant differences between the control and AI-2 or between AI-2 and furanone compound-treated groups were analyzed. A p value of <0.05 was considered statistically significant.

Acknowledgments

This study was supported by a grant (HI12C0675) from the Korea Healthcare Technology R&D, Ministry of Health and Welfare, Republic of Korea.

Appendix A. Supplementary data

Supplementary data related to this article can be found at http://dx.doi.org/10.1016/j.ejmech.2017.05.037.

References

[1] P. Albuquerque, A. Casadevall, Quorum sensing in fungi–a review, Med. Mycol. 50 (2012) 337–345.
[2] W.C. Fuqua, S.C. Winans, E.P. Greenberg, Quorum sensing in bacteria: the LuxR-LuxI family of cell density-responsive transcriptional regulators, J. Bacteriol. 176 (1994) 269.
[3] M.E. Taga, B.L. Bassler, Chemical communication among bacteria, Proc. Natl. Acad. Sci. 100 (2003) 14549–14554.
[4] W.R. Galloway, J.T. Hodgkinson, S.D. Bowden, M. Welch, D.R. Spring, Quorum sensing in Gram-negative bacteria: small-molecule modulation of AHL and AI-2 quorum sensing pathways, Chem. Rev. 111 (2010) 28–67.
[5] J.W. Costerton, P.S. Stewart, E.P. Greenberg, Bacterial biofilms: a common cause of persistent infections, Science 284 (1999) 1318–1322.
[6] A.K. Bhardwaj, K. Vinothkumar, N. Rajpara, Bacterial quorum sensing inhibitors: attractive alternatives for control of infectious pathogens showing multiple drug resistance, Recent Pat. Antiinfect. Drug Discov. 8 (2013) 68–83.
[7] M.J. Federle, Autoinducer-2-based chemical communication in bacteria: complexities of interspecies signaling in: bacterial Sensing and Signaling, Karger Publ. 16 (2009) 18–32.
[8] A.H. Rickard, R.J. Palmer, D.S. Blehert, S.R. Campagna, M.F. Semmelhack, P.G. Egland, B.L. Bassler, P.E. Kolenbrander, Autoinducer 2: a concentration-dependent signal for mutualistic bacterial biofilm growth, Mol. Microbiol. 60 (2006) 1446–1456.
[9] S. Schauder, K. Shokat, M.G. Surette, B.L. Bassler, The LuxS family of bacterial autoinducers: biosynthesis of a novel quorum-sensing signal molecule, Mol. Microbiol. 41 (2001) 463–476.
[10] A. Jayaraman, T.K. Wood, Bacterial quorum sensing: signals, circuits, and implications for biofilms and disease, Annu. Rev. Biomed. Eng. 10 (2008) 145–167.
[11] B.J. Paster, I. Olsen, J.A. Aas, F.E. Dewhirst, The breadth of bacterial diversity in the human periodontal pocket and other oral sites, Periodontol 2000 (42) (2006) 80–87.
[12] P.E. Kolenbrander, R.N. Andersen, D.S. Blehert, P.G. Egland, J.S. Foster, R.J. Palmer, Communication among oral bacteria, Microbiol. Mol. Biol. Rev. 66 (2002) 486–505.
[13] P.D. Marsh, M.V. Martin, M.A. Lewis, D. Williams, Oral Microbiology, Elsevier Health Sciences, 2009.
[14] J. Frias, E. Olle, M. Alsina, Periodontal pathogens produce quorum sensing signal molecules, Infect. Immun. 69 (2001) 3431–3434.
[15] P.E. Kolenbrander, R.J. Palmer, S. Periasamy, N.S. Jakubovics, Oral multispecies biofilm development and the key role of cell–cell distance, Nat. Rev. Microbiol. 8 (2010) 471–480.
[16] D.J. Bradshaw, P.D. Marsh, G.K. Watson, C. Allison, Role of Fusobacterium nucleatum and coaggregation in anaerobe survival in planktonic and biofilm oral microbial communities during aeration, Infect. Immun. 66 (1998) 4729–4732.
[17] P.E. Kolenbrander, R.J. Palmer, A.H. Rickard, N.S. Jakubovics, N.I. Chalmers, P.I. Diaz, Bacterial interactions and successions during plaque development, Periodontol 2000 (42) (2006) 47–79.
[18] K. Hojo, S. Nagaoka, T. Ohshima, N. Maeda, Bacterial interactions in dental biofilm development, J. Dent. Res. 88 (2009) 982–990.
[19] T. Okuda, E. Kokubu, T. Kawana, A. Saito, K. Okuda, K. Ishihara, Synergy in biofilm formation between Fusobacterium nucleatum and Prevotella species, Anaerobe 18 (2012) 110–116.
[20] Y.-J. Jang, Y.-J. Choi, S.-H. Lee, H.-K. Jun, B.-K. Choi, Autoinducer 2 of Fusobacterium nucleatum as a target molecule to inhibit biofilm formation of periodontopathogens, Arch. Oral Biol. 58 (2013) 17–27.
[21] D.G. Cvitkovitch, Y.-H. Li, R.P. Ellen, Quorum sensing and biofilm formation in Streptococcal infections, J. Clin. Invest. 112 (2003) 1626–1632.
[22] T.B. Rasmussen, M. Manefield, J.B. Andersen, L. Eberl, U. Anthoni, C. Christophersen, P. Steinberg, S. Kjelleberg, M. Givskov, How Delisea pulchra furanones affect quorum sensing and swarming motility in Serratia liquefaciens MG1, Microbiology 146 (2000) 3237–3244.
[23] M. Hentzer, M. Givskov, Pharmacological inhibition of quorum sensing for the treatment of chronic bacterial infections, J. Clin. Invest. 112 (2003) 1300–1307.
[24] J. Pan, D. Ren, Quorum sensing inhibitors: a patent overview, Expert Opin. Ther. Pat. 19 (2009) 1581–1601.
[25] M. Hentzer, H. Wu, J.B. Andersen, K. Riedel, T.B. Rasmussen, N. Bagge, N. Kumar, M.A. Schembri, Z. Song, P. Kristoffersen, Attenuation of Pseudomonas aeruginosa virulence by quorum sensing inhibitors, EMBO J. 22 (2003) 3803–3815.
[26] J. Lönn-Stensrud, F. Petersen, T. Benneche, A.A. Scheie, Synthetic bromated furanone inhibits autoinducer-2-mediated communication and biofilm formation in oral streptococci, Oral Microbiol. Immunol. 22 (2007) 340–346.
[27] H. Wu, Z. Song, M. Hentzer, J.B. Andersen, S. Molin, M. Givskov, N. Høiby, Synthetic furanones inhibit quorum-sensing and enhance bacterial clearance in Pseudomonas aeruginosa lung infection in mice, J. Antimicrob. Chemother. 53 (2004) 1054–1061.
[28] S. Yang, O.A. Abdel-Razek, F. Cheng, D. Bandyopadhyay, G.S. Shetye, G. Wang, Y.-Y. Luk, Bicyclic brominated furanones: a new class of quorum sensing modulators that inhibit bacterial biofilm formation, Bioorg. Med. Chem. 22 (2014) 1313–1317.
[29] T. Zang, B.W. Lee, L.M. Cannon, K.A. Ritter, S. Dai, D. Ren, T.K. Wood, Z.S. Zhou, A naturally occurring brominated furanone covalently modifies and inactivates LuxS, Bioorg. Med. Chem. Lett. 19 (2009) 6200–6204.
[30] J.C. Janssens, H. Steenackers, S. Robijns, E. Gellens, J. Levin, H. Zhao, K. Hermans, D. De Coster, T.L. Verhoeven, K. Marchal, Brominated furanones inhibit biofilm formation by Salmonella enterica serovar Typhimurium, Appl. Environ. Microbiol. 74 (2008) 6639–6648.
[31] H.P. Steenackers, J. Levin, J.C. Janssens, A. De Weerdt, J. Balzarini, J. Vanderleyden, D.E. De Vos, S.C. De Keersmaecker, Structure–activity relationship of brominated 3-alkyl-5-methylene-2 (5H)-furanones and alkylmaleic anhydrides as inhibitors of Salmonella biofilm formation and quorum sensing regulated bioluminescence in Vibrio harveyi, Bioorg. Med. Chem. 18 (2010) 5224–5233.
[32] S.G. Newman, V. Aureggi, C.S. Bryan, M. Lautens, Intramolecular cross-coupling of gem-dibromoolefins: a mild approach to 2-bromo benzofused heterocycles, Chem. Commun. (2009) 5236–5238.
[33] L. Eberson, L. Landström, Studies on cyclic anhydrides IV. Rate constants for the hydrolysis of some cyclic anhydrides exhibiting ring strain, Acta Chem. Scand. 26 (1972) 239.
[34] F. De Nanteuil, E. Serrano, D. Perrotta, J. Waser, Dynamic kinetic asymmetric [3+ 2] annulation reactions of aminocyclopropanes, J. Am. Chem. Soc. 136 (2014) 6239–6242.
[35] A. Allahdad, D.W. Knight, An investigation of the Wittig reaction between a series of mono-substituted phthalic anhydrides and ethoxycarbonylmethyl idenetri- phenylphosphorane, J. Chem. Soc. Perkin Trans. I (1982) 1855.
[36] W.-L. Ng, B.L. Bassler, Bacterial quorum-sensing network architectures, Annu. Rev. Genet. 43 (2009) 197.
[37] D. Martinelli, G. Grossmann, U. Séquin, H. Brandl, R. Bachofen, Effects of natural and chemically synthesized furanones on quorum sensing in Chromobacterium violaceum, BMC Microbiol. 4 (2004) 1.
[38] K.M. Smith, Y. Bu, H. Suga, Library screening for synthetic agonists and antagonists of a Pseudomonas aeruginosa autoinducer, Chem. Biol. 10 (2003) 563–571.
[39] L. Yujie, X. Geng, Y.-c. Huang, Y. Li, K. Yang, L. Ye, X. Chen, G. Zhao, C. Yin, The effect of brominated furanones on the formation of Staphylococcus aureus biofilm on PVC, Cell Biochem, Biophys. 67 (2013) 1501–1505.
[40] M. Guo, S. Gamby, Y. Zheng, H.O. Sintim, Small molecule inhibitors of AI-2 signaling in bacteria: state-of-the-art and future perspectives for anti-quorum sensing agents, Int. J. Mol. Sci. 14 (2013) 17694–17728.
[41] H. Shao, D. James, R.J. Lamont, D.R. Demuth, Differential interaction of aggregatibacter (actinobacillus) actinomycetemcomitans LsrB and RbsB proteins with autoinducer 2, J. Bacteriol. 189 (2007) 5559–5565.
[42] D. James, H. Shao, R.J. Lamont, D.R. Demuth, The Actinobacillus actinomycetemcomitans ribose binding protein RbsB interacts with cognate and heterologous autoinducer 2 signals, Infect. Immun. 74 (2006) 4021–4029.
[43] P.-F. Liu, W. Shi, W. Zhu, J.W. Smith, S.-L. Hsieh, R.L. Gallo, C.-M. Huang, Vaccination targeting surface FomA of Fusobacterium nucleatum against bacterial co-aggregation: implication for treatment of periodontal infection and halitosis, Vaccine 28 (2010) 3496–3505.
[44] R. Huang, M. Li, R.L. Gregory, Bacterial interactions in dental biofilm, Virulence 2 (2011) 435–444.